Groundwater geochemistry and hydrochemical processes in the Egbako aquifer, Northern Bida Basin, Nigeria

Geoquímica e processos hidroquímicos de águas subterrâneas no aquífero Egbako, Bacia de Bida do Norte, Nigéria

Abdulwahid Kolawole Aweda[1,2] , **Benson Shadrach Jatau[1]** & **Nathaniel Gotar Goki[1]**

[1]Nasarawa State University, Keffi, Nigeria
[2]Ibrahim Badamasi Babangida University, Lapai, Nigeria
E-mails: awedaka@yahoo.com (AKA), sj.blanson@gmail.com (BSJ), nathgoki@gmail.com (NGG)

ABSTRACT

Thirty-five groundwater samples from the aquifer were collected and analyzed for major cations and anions to understand the groundwater chemistry and hydrochemical processes in the Egbako aquifer. Laboratory studies identified the major ions while the results were analyzed using different graphical methods and ionic plots. The abundance of the major cations and anions are $Ca^{2+}>K^+>Na^+>Mg^{2+}$ and $HCO_3^->NO_3^->Cl^->SO_4^{2-}$ respectively. The dominant hydrochemical facies are calcium-bicarbonate ($Ca-HCO_3$), sodium-bicarbonate ($Na-HCO_3$) and mixed calcium-sodium bicarbonate ($Ca-Na-HCO_3$) water types. Interpretation of bivariate and scatter plots indicate silicate weathering, simple dissolution and ion exchange as the dominant processes in the aquifer. Saturation indices reveals evaporites (halite, gypsum and anhydrite) undersaturation, supersaturation in most samples with respect to silicates (quartz and kaolinite) and few samples for carbonate (calcite, aragonite, dolomite). Assessment of the water quality indicate that they are chemically suitable for human consumption except in the agricultural fields of southwestern areas where high nitrate concentration is present.

Keywords: Water quality; Saturation index; Groundwater evolution; Bida Basin; Hydrochemical processes.

RESUMO

Trinta e cinco amostras de água subterrânea do aquífero foram coletadas e analisadas para os principais cátions e ânions para entender a química e os processos hidroquímicos das águas subterrâneas no aquífero Egbako. Estudos laboratoriais identificaram os íons majoritários, enquanto os resultados foram analisados usando diferentes métodos gráficos e gráficos iônicos. A abundância dos cátions e ânions majoritários foram, respectivamente, $Ca^{2+}>K^+>Na^+>Mg^{2+}$ e $HCO_3^->NO_3^->Cl^->SO_4^{2-}$. As fases hidroquímicas dominantes são os tipos de água bicarbonato de cálcio (Ca-HCO3), bicarbonato de sódio (Na-HCO3) e bicarbonato de cálcio e sódio misto (Ca-Na-HCO3). A interpretação de gráficos bivariados e de dispersão indica o intemperismo do silicato, a dissolução simples e a troca iônica como os processos dominantes no aquífero. Os índices de saturação revelam subsaturação de evaporitos (halita, gesso e anidrita), supersaturação na maioria das amostras em relação aos silicatos (quartzo e caulinita) e poucas amostras de carbonato (calcita, aragonita, dolomita). A avaliação da qualidade da água indica que elas são quimicamente adequadas para o consumo humano, exceto nos campos agrícolas das áreas do sudoeste, onde há alta concentração de nitrato.

Palavas-chave: Qualidade da água; Índice de saturação; Evolução das águas subterrâneas; Bacia Bida; Processos hidroquímicos.

INTRODUCTION

Reliance on groundwater in many countries of the world, especially in the Sub-Saharan African areas for domestic, agricultural and industrial use has continued to increase over several decades. Rapid population growth and urbanization, industrialization, irrigation use and inability of existing water infrastructure has led to this increased groundwater development (Xu et al., 2022; Nsabimana & Li, 2023). The demand for safe water has put a lot of stress on the available groundwater resource resulting in over exploitation in most areas and thus putting the quality at risk of contamination (Li et al., 2023; Nsabimana et al., 2023). An understanding of the hydrogeological and hydrogeochemical properties of an aquifer is important in groundwater evaluation and management (Ren et al., 2021). Hydrogeochemical processes that are responsible for altering the chemical composition of groundwater vary with respect to space and time.

Chemical characteristics of groundwater play an important role in assessing and classifying the quality of water (Fijani et al., 2017). The quality of groundwater is determined by its physical, chemical and biological properties, which all depends on the natural and anthropogenic influences within the subsurface environment (Owor et al., 2021). Its quality may become altered along its flow path through a cumulative consequence of processes which includes rock-water interaction, dissolution of soluble mineral species, evaporation, transpiration, selective uptake by vegetation, redox reaction, mineral dissociation, precipitation of secondary minerals, mixing of waters, chemical fertilizers and biological processes (Appelo & Postma, 1993; Tarawneh et al., 2019). Proper understanding of the geochemical processes controlling groundwater chemical composition is important in understanding the hydrochemical framework which is useful for sustainable and effective development of groundwater resources in an area (Srinivasamoorthy et al., 2014; Tarawneh et al., 2019).

Recent research on groundwater quality and hydrochemical processes has largely focused on their spatial and temporal distribution (Zhou et al., 2022; Mu et al., 2023; Xu et al., 2023) using statistical tools (Nsabimana & Li, 2023), background and threshold values of groundwater composition, and how hydrochemical processes affect fractionation of environmental isotopes (He et al., 2022). Xu et al. (2023) assessed the risk of nitrate in drinking water to human health using the spatial distribution of the major indicators of the water quality while also understanding the processes controlling the hydrochemistry of the groundwater in the Guanzhong Basin. Nsabimana and Li (2023) developed an industrial water quality index (IndWQI) utilized a combination of statistical, ionic plots and correlation analysis on results of water chemistry in order to assess the water quality and its suitability for industrial usage in Guanzhong Basin of China. Sources of groundwater pollution from the Malian River and their level of impact was studied by Mu et al. (2023) while evaluating spatiotemporal change in water quality over time using ANOVA and cluster analysis on the water quality parameters. Zhou et al. (2022) in their study of groundwater in Xi'an Region of China established spatiotemporal changes in the natural background level and threshold values of all measured ions in the groundwater with time. A Recent study by He et al. (2022) in a fracturing field revealed that hydrochemical processes have

little effect on isotopes of strontium ($^{87}Sr/^{86}Sr$) when fracturing flowback water mixes with groundwater.

The study area sits in the northern Bida Basin where groundwater provides over 80% of water need for domestic and agricultural activities. Previous hydrogeological studies here have focused on estimating the depth to aquifer and their hydraulic properties (Idris-Nda, 2012; Olabode et al., 2012; Idris-Nda et al., 2013) as well as assessing the groundwater quality and their suitability for human consumption (Idris-Nda et al., 2016; Sidi et al., 2016; Amadi et al., 2017; Ashafa et al., 2020). Findings from these studies revealed elevated concentration of nitrate and sulphate arising from intensive use of agrochemicals for agricultural and anthropogenic activities, with no study focused on understanding the relationship between the hydrochemistry and processes influencing them. The aim of this study is to understand the groundwater hydrochemistry and hydrochemical processes within the Ebgbako Aquifer of the Bida Basin. Classical hydrochemical methods which include facies analysis, ionic relationship between major ions and saturation indices are used to understand the processes influencing the groundwater chemistry. It also presents an understanding of the mechanism controlling the groundwater chemistry, pollution sources and delineates the groundwater types in the study area which will be useful in future groundwater management and decision making.

STUDY AREA AND DESCRIPTION

Location

The study area is Egbako Sheet 183 SW and is bounded by Latitude 9º0'N to 9º15'N and Longitude 5º30'E to 5º45'E. It is part of the northern sector of the Bida Basin of Central Nigeria. The basin trends in a northwest-southeast direction with the Basement Complex marking its northwest boundary while the Anambra Basin is the boundary to the southeast (Obaje, 2009). It is a heavily agricultural area that relies on groundwater especially for processing farm produce and domestic consumption.

Climate and topography

The study area is part of the southern Guinea Savannah climate zone of Nigeria having a mean annual rainfall of 1000mm and 1200mm (Anurunwa et al., 2020) with average temperature of 30°C (Suleiman, 2014). The area has a hilly topography in most part with surface elevation of between 277 m and 161 m above mean sea level (Figure 1). The high elevation is predominant in the southeastern and northwestern, providing the main aquifer recharge in the area. The main streams are flowing in the southwest and northeast direction respectively, draining other minor streams in a dendritic pattern which is controlled by the topography of the study area (Aweda et al., 2023).

Geological setting

The study area is part of the roughly elliptical NW-SE trending intracratonoc Bida Basin which stretches northwards
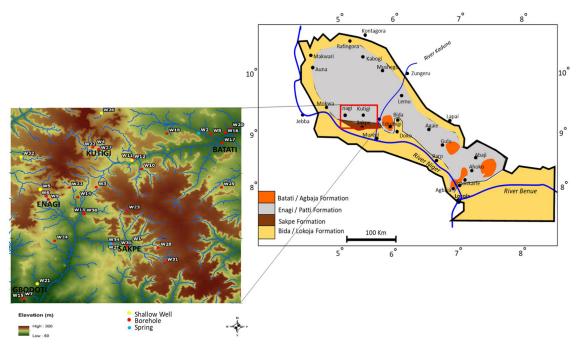
Figure 1. Location and Geology of the Study Area (Obaje et al., 2019).

from the Niger-Benue River confluence at Lokoja to the basement complex in which marks its northwest extent, separating it from the Early Cretaceous to Late Jurassic Illo and Gundumi Formations of the Sokoto Basin (Rahaman et al., 2019). The regional geology of the Bida Basin has been studied in details by (Adeleye, 1974; Kogbe et al., 1983; Olaniyan & Olobaniyi, 1996; Obaje, 2009; Rahaman et al., 2019). The geological map of the area is shown in Figure 1. Outcropping sections of rocks from all formations are present in the study area with age ranging from Campanian to Maastrichtian. The Campanian series are the Bida Sandstone Formation and the Sakpe Ironstone Formation. The former formation is composed of a basal conglomeratic sandstone and fines upward into medium-grained sandstone, siltsone and subordinate claystone, covering most of the basal areas and is the dominant exposed formation.

The Sakpe Formation outcrops in the southeastern part of the study area and is predominantly oolitic and pisolitic ironstone band (Obaje, 2013), above and below a silt to mudstone unit with concretions at the top. The Lower Maastrichtian Enagi Formation outcrops dominantly in the northwest of the area and it lithologically comprises of clayey siltstone and sandstone which gets coarser upward (Rahaman et al., 2019). The Upper Maastrichtian Batati Formation are generally massive oolitic ironstones forming sharp contact with the underlying Enagi Formation (Adeleye, 1974).

Hydrogeology

Egbako aquifer consists of sandstones from Bida and Enagi Formations of the Northern Bida Basin and is developed to provide groundwater for agricultural and domestic use. Groundwater development records are very scarce in the study area. The Maastrichtian Enagi Formation constitutes the most

important regional aquifer system in the area as it contains many aquiferous layers that are confined by clayey lenses (Kehinde, 1993). The basal sandstone and conglomerates of the Bida Formation are also aquiferous, but with low transmissivity because they are highly consolidated.

Alluvial aquifers are also present and are associated with the River Niger course. In one study by (Idris-Nda et al., 2014), the northern Bida Basin was reported to be composed of four aquifers occurring a depth of between 30 and 100 meters. The aquifer transmissivity is very low with values of between 5 and 29.3m³/day (Mands, 1992; Kehinde, 1993) to over 50m³/day locally indicating high heterogeneity and anisotropy of the aquifer system (Kehinde, 1993). The alluvial aquifers have variable texture and composition with thickness that rarely exceed 30 meters and are recharged directly by rainfall and adjoining flood waters of the river systems (Offodile, 2013). Confined, unconfined, phreatic and free flowing groundwater conditions occur within the basin with estimated annual groundwater recharge of not more than 228.8mm (Kehinde, 1993).

METHODOLOGY

Representative groundwater samples were collected from 35 shallow/ hand-dug wells (5 samples), boreholes (28) and springs (2) on the basis of geographic distribution during June, 2021 (Figure 1). The selected points are active wells used for domestic purposes and processing of farm produce, with depths between 30 meters and 100 meters. The water samples were collected in 500mL polyethene bottles that had been soaked in 10% nitric acid and rinsed with distilled water prior to sampling. The groundwater samples collected were stored at a temperature of 4°C. On field measurements of pH, Electrical conductivity

(Ec), temperature and total dissolved solids (TDS) were made using a digital conductivity and pH meter immediately after sampling.

Chemical analysis was conducted at the Laboratory for Geology and Applied Hydrogeology of Ghent University. Major ions (Na, K) were determined using the ICP-MS, while calcium (Ca), carbonate (CO_3), bicarbonate (HCO_3), and chloride (Cl) were analyzed by the volumetric methods. Magnesium (Mg) was calculated from the total hardness (TH) and calcium composition, while sulfate (SO_4) was estimated using colorimetry. Concentration of phosphate (PO_4), Nitrate (NO_3), Iron (Fe_2 and Fe_3) were determined using spectrophotometer.

The ionic balance error between the total cations (Na^+, Ca^{2+}, Mg^{2+}, $Fe^{2+}+Fe^{3+}$ and Mn^{2+}) and anions (Cl^-, SO_4^{2-}, NO_3^-, HCO_3^- and PO_4^{2-}) in milliequivalent per liter (meq/L) for the result of the chemical analysis was determined for each sample using the formulae:

$$ionic\ balance\ error = \frac{\Sigma(Cations) - \Sigma(anions)}{\Sigma(Cations) + \Sigma(anions)} X 100 \qquad (1)$$

The ionic balance error for all the results was between the acceptable limit of $\pm 5\%$

The hydrochemical analysis was carried out using Piper and Dorov plots on Grapher 14 software while saturation indices (SI) of the common mineral phases (Carbonate, evaporite, silicate) present in groundwater were calculated using the hydrogeochemical equilibrium model, Phreeqc Interactive 3.7.3 software. MS excel was used for preparing the base ion plots used in this study.

RESULTS AND DISCUSSION

Physicochemical parameters of groundwater

The chemical composition of important chemical constituents of the groundwater samples is presented in box and whiskers plot (Figure 2) while a statistical summary is presented in Table 1. The wide ranges and as well as high standard deviation for some of the parameters indicate that the chemical composition of the water is affected by various processes which could include rock-water interaction and anthropogenic influence (Srinivasamoorthy et al., 2014). The average value of the pH is 6.0 and varies from 5.6 to 6.6 indicating slightly acidic condition. This is possibly resulted from release of H_3O^+ as groundwater flows through the upper clay layer confining the aquifer, resulting to higher concentration of H^+ (Zhou et al., 2015).

The TDS shows a wide range of 13.4 to 351.3 and an average of 57.0 indicating a large degree of variation (64.65%) in the water quality. The groundwater samples are considered to be fresh since their values are below 1000mg/L for classification, and 500mg/L permissible for drinking water.

The mean content of cations and anions in the study area shows $Ca^{2+} > K^+ > Na^+ > Mg^{2+}$ and $HCO_3^- > NO_3^- > Cl^- > SO_4^{2-} > NO_2^-$ in milligram per liter respectively. This content is a good indicator for potability of groundwater when compared with the corresponding standards of the (World Health Organization, 2022) guidelines.

For the cations, the concentration of Ca^{2+} varies from 0.96mg/L to 32.8mg/L with average of 5.6mg/L, while K^+
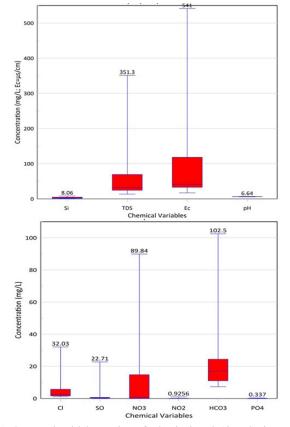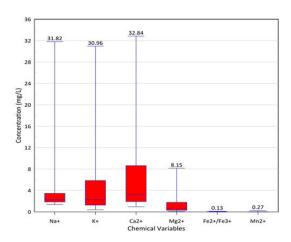

Figure 2. Box and Whiskers Plot of Physical and Chemical Parameters.

Table 1. Statistical Chemical analysis of the Studied Groundwater Samples (All parameters in mg/L except Ec in μs/cm; SI and pH are dimensionless MIN=Minimum; MAX=Maximum; MEAN=Average; STD=Standard Deviation).

Parameters	Borehole				Shallow Well				Spring			
	MIN	MAX	MEAN	STD	MIN	MAX	MEAN	STD	MIN	MAX	MEAN	STD
Na^+	1.40	31.82	3.78	5.56	1.54	9.41	4.10	3.63	1.67	1.85	1.76	0.13
K^+	0.39	30.96	5.44	7.36	0.67	15.59	5.18	6.98	0.67	2.37	1.52	1.20
Ca^{2+}	0.96	32.84	5.18	6.51	3.54	14.55	8.78	5.52	1.58	9.43	5.50	5.55
Mg^{2+}	0.07	8.15	1.26	1.75	0.43	6.45	2.43	2.83	0.21	1.78	0.99	1.11
Na^+	1.40	31.82	3.78	5.56	1.54	9.41	4.10	3.63	1.67	1.85	1.76	0.13
K^+	0.39	30.96	5.44	7.36	0.67	15.59	5.18	6.98	0.67	2.37	1.52	1.20
Fe^{2+}/Fe^{3+}	0.00	0.11	0.04	0.03	0.01	0.13	0.05	0.06	0.02	0.05	0.04	0.02
Mn^{2+}	0.00	0.27	0.02	0.05	0.00	0.05	0.02	0.02	0.00	0.01	0.00	0.00
NH^{4+}	0.00	0.95	0.18	0.19	0.32	0.43	0.37	0.04	0.14	0.34	0.24	0.14
HCO_3^-	7.32	102.48	20.61	18.20	9.76	22.57	17.39	5.42	9.76	48.80	29.28	27.61
Cl^-	1.05	32.03	5.01	6.62	1.04	19.42	7.67	8.56	1.57	1.87	1.72	0.21
SO_4^{2-}	0.02	22.72	1.63	4.36	0.05	11.35	2.95	5.60	0.02	0.20	0.11	0.13
NO_3^-	0.00	89.84	12.07	22.28	0.00	73.37	27.94	34.90	0.00	0.00	0.00	0.00
NO_2^-	0.00	0.93	0.06	0.18	0.00	0.07	0.02	0.03	0.00	0.00	0.00	0.00
pH	5.56	6.64	6.02	0.24	5.96	6.25	6.11	0.14	5.90	6.37	6.14	0.33
TDS	13.37	351.33	55.30	67.72	29.97	152.30	76.96	58.48	16.12	66.56	41.34	35.66
SI	0.50	8.06	2.86	1.97	2.07	6.76	3.59	2.15	1.10	1.25	1.18	0.11
Ec	17.00	541.00	84.36	106.87	38.30	264.00	127.60	109.97	23.00	83.00	53.00	42.43
Quartz	-4.21	1.08	-0.93	1.21	-1.02	1.91	-0.01	1.31	-0.06	0.03	-0.02	0.06
Kaolinite	-8.86	2.99	-0.32	1.82	-1.21	4.66	0.81	2.62	0.71	0.89	0.80	0.13
Anhydrite	-6.62	-0.29	-5.22	1.17	-6.14	-3.32	-5.03	1.23	-5.89	-3.46	-4.68	1.72
Aragonite	-4.80	1.29	-3.52	1.12	-3.60	-2.83	-3.21	0.33	-4.25	0.51	-1.87	3.37
Calcite	-4.65	1.43	-3.37	1.12	-3.45	-2.68	-3.07	0.33	-4.10	0.66	-1.72	3.37
Dolomite	-9.84	2.39	-7.15	2.27	-7.46	-5.38	-6.55	0.86	-8.75	0.73	-4.01	6.70
Gypsum	-6.32	0.01	-4.91	1.17	-5.83	-3.02	-4.73	1.22	-5.59	-3.15	-4.37	1.73
Halite	-10.30	-7.28	-9.54	0.73	-10.26	-4.86	-8.64	2.53	-9.58	-9.06	-9.32	0.37

concentration is between 0.39mg/L and 30.96mg/L with average of 5.19mg/L (Table 1). The origin of Ca^{2+} in groundwater are believed to be from minerals rich in calcium such as calcite, aragonite, dolomite, silicate minerals and inorganic fertilizers that find their way into groundwater from infiltration and subsurface flow (Prasanna et al., 2010; Nematollahi et al., 2018). Similarly, potassium bearing minerals such as clay minerals, fertilizer and domestic wastes are believed to be the source of K^+ in groundwater (Prasanna et al., 2010; Nematollahi et al., 2018).

The concentrations of Ca and K are within the permissible (World Health Organization, 2022) limit for drinking water quality. The average concentration of Na^{2+} is 3.70mg/L with a range of 1.4mg/L and 31.8mg/L while Mg^{2+} has range of 0.1mg/L and 8.2mg/L with average of 1.4mg/L (Table 1). Dissolution and breakdown of Sodium bearing minerals such as halite and sodium feldspars, as well as from human sources such as industrial, domestic and animal wastes can be the main sources of Na in groundwater (Nematollahi et al., 2018). The concentrations of both Na and Mg are also below the maximum permissible (World Health Organization, 2022) limits for drinking water quality.

Alkalinity of water, measured by its bicarbonate concentration, is the measure of its ability of neutralization or its ability to resist acidification (Srinivasamoorthy et al., 2014). Bicarbonates (HCO_3) has the highest concentration among the anions with value of 7.32mg/L to 102.48ng/L and average of 20.74mg/L, placing all the water samples within the 300mg/L threshold for bicarbonate in groundwater (World Health Organization, 2022). Bicarbonates in groundwater is mainly from dissolution of silicates and rocks as well as atmospheric CO_2 and CO_2 released from decomposition of organic contents in soil.

The concentration of NO_3^- is between 0 and 89.84mg/L and average of 13.20mg/L. Although about 50% of the samples have no traces of NO_3^- in them, 12% have concentration above the maximum permissible limit of 45mg/L for drinking water (Table 1). These high concentrations are generally from anthropogenic sources which include agricultural chemicals and sewage. 75% of the samples with concentration above the permissible limit are in areas with very high agricultural activities while 25% are within high surface waste disposal areas.

The Cl^- has concentration from 1.04mg/L to 32.03mg/L with mean value of 5.13mg/L, also placing them within the safe limit of 250mg/L recommended for drinking water (World Health Organization, 2022). Chlorides are naturally occurring in all water types and sourced from rainwater, inorganic fertilizers and sewage. The sulphate (SO_4^{2-}) content ranges from 0.02mg/L to 22.72mg/L and has an average of 1.69mg/L. In all the groundwater samples, sulphate is within the safe limit of 200mg/L permissible for human consumption. Sulphate in groundwater mainly results from fertilizers, municipal wastes and dissolution of filtering waters.

Silica concentration in groundwater is between 0.50mg/L and 8.06mg/L with mean concentration of 2.85mg/L. Solubility of silica in water is enhanced by the presence of an alkaline

environment and weathering of silicate minerals from existing rocks (Srinivasamoorthy et al., 2009).

Hydrochemical facies analysis

Groundwater and aquifer minerals interactions are important for understanding the groundwater genesis and also affects the water chemistry (Srinivasamoorthy et al., 2014). Characterization of groundwater hydrogeochemical evaluation can be done with the aid of a trilinear diagram of (Piper, 1944), which is composed of three different fields; two triangular fields on the lower sides to plot the cations (left side) and anions (right sides) while the third is a diamond shaped field on which the intercepts of the cation and anion projections are plotted, allowing for the characterization of the hydrogeochemical evolution of the groundwater based on the field they fall in on the diagram.

On the trilinear diagram (Figure 3), 62% of the water samples fall within the central part on the cation triangle, 29% on the lower right corner, while 9% falls within the lower left of the triangle. This means there is no dominant cation in 62% of the water, Na^+ is the dominant ion in 29% and Ca^+ in 9% of the water.

On the anion triangle, 66% of the groundwater samples plotted to the left which signifies a high concentration of HCO_3^- ion in the groundwater while the other 34% plotted in the lower right of the triangle indicating dominance of Cl^- and NO_3^- over other anions in them.

34% of the groundwater sampling points, which includes all spring samples, falls in the left side (zone-1) of the diamond-shaped field, characterizing them as calcium-bicarbonate ($Ca-HCO_3$) facies indicating that this groundwater is recharged largely from rainfall and further suggesting that secondary alkalinity exceeds 50% (Tarawneh et al., 2019). About 50% of the samples fall within the mixing zone (zone-5, mixed facies), with mixed Ca-Na-HCO_3 and mixed Ca-Mg-Cl as the water types in the lower and upper mixing zones respectively, indicating increasing rock-water interaction with none of the cations or anions controlling
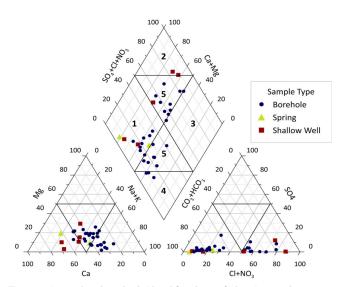
its chemical composition. These waters are recent recharge waters which exhibit simple mixing or dissolution without any dominant anion or cation (Lloyd & Heathcote, 1985). 9% of the water samples fall within the sodium-bicarbonate (Na-HCO_3, zone-4) facies pointing to possible anthropogenic influence, especially from sewage, chemical fertilizers and other agro-chemicals along the groundwater flow path. Two of the shallow well samples (6%) are calcium chloride (Ca-Cl, zone-2) water types with no carbonate hardness exceeding 50% in them, suggesting anthropogenic pollution by NO_3^-, expectedly as they are unprotected wells.

Saturation index

Saturation index (SI) is used to evaluate how much equilibrium exist between water and the minerals present in them, defining the intensity of soluble minerals. This is useful in predicting thermodynamic controls on the composition of the groundwater (Deutsch, 1997). Understanding the saturation states of minerals is useful in understanding the various phases of hydrochemical evolution as well as determining the chemical reactions responsible for controlling the water chemistry (Nematollahi et al., 2018). SI is the ratio of the ion activity product (log IAP) and the solubility product (log KT) of the mineral, the result of which predicts the trend of mineral equilibrium in water as well as water-rock interaction (Zhang et al., 2020).

If SI is zero, the water is saturated with respect to the particular mineral. SI of less than zero indicate an under-saturated state (dissolution) with respect to the particular mineral and could reflect the character of water originating from rocks not having sufficient amount of the mineral for solution or having quick infiltration. Such mineral will continue to be weathered by the groundwater (Zhang et al., 2020). SI greater than zero suggests oversaturated state (precipitation) with respect to the particular mineral phase (Rao, 2017) and incapable of dissolving more of the mineral. Oversaturation reflects groundwater originating from an aquifer having ample amount of the mineral with good resident time to reach equilibrium (Aghazadeh & Mogaddam, 2011). There could however be significant change in alkalinity and corresponding SI values over time. As such water with SI close to zero (between -0.5 and +0.5) would be close to being neutral, and therefore the water will have no tendency to dissolve or precipitate the mineral (Haile-Meskale, 2017), representing an equilibrium state of the mineral phase (Zhang et al., 2020).

A summary of the SI values of the minerals in groundwater as determined by PHREEQC interactive software is presented in Table 1. Mean saturation index of anhydrite, aragonite, calcite, dolomite, gypsum, halite, quartz and kaolinite are -5.17, -3.39, -3.24, -6.90, -4.86, -9.44, -0.35 and 0.13 respectively (Table 1). Plots of the SI against TDS for all the analyzed water are presented in Figure 4. Evaporites (halite, gypsum and anhydrite) are entirely undersaturated largely because the major lithological units in the area are silici-clastic rocks having insufficient evaporite minerals for solution.

Of the carbonate minerals (aragonite, calcite and dolomite) only two samples (6%) are oversaturated with all the minerals while all others are undersaturated. This means that the groundwater will generally dissolve these minerals with the exception of the two
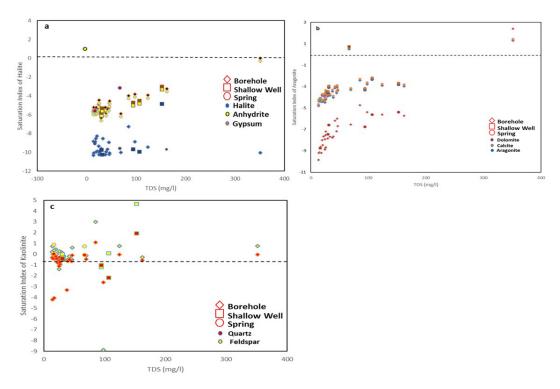

Figure 3. Hydrochemical Classification of the Groundwater on the Piper Trilinear Diagram.

Figure 4. Saturation Indices for Evaporites (a); Carbonate (b); and Silicate (c) Mineral Phases.

samples which will precipitate them due to evaporation. Fourteen samples (40%) are saturated with quartz and 17 samples (48.6%) with kaolinite which indicate that the groundwater here will neither dissolve nor precipitate these silicate minerals as the mineral phases are in a state of equilibrium. Twenty-three and twenty-eight percent of the samples are over saturated and undersaturated in kaolinite respectively while fifty-four percentage and six percent of samples are undersaturated and oversaturated with quartz respectively. This suggests that silicate mineral phases played important roles in regulating the groundwater chemistry in the area.

Natural processes controlling hydrochemistry

Gibbs diagram (Gibbs, 1970) is used to describe the natural mechanisms that controls groundwater chemistry in relation to the influences of atmospheric rainwater (precipitation), mineral dissolution and weathering (lithology and/or soil) as well as climate (evaporation) and fractional crystallization (Tarawneh et al., 2019).

The diagram consists of a plot of $Na^+ + K^+/Na^+ + K^+ + Ca^{2+}$ against TDS and $Cl^-/Cl^- + HCO_3^-$ against TDS. The Gibbs diagram for the sampled locations is presented in Figure 5. Most of the samples fall within the precipitation dominance side, indicating that atmospheric precipitation is the major controlling factor of the groundwater chemistry in most part. The dominance of atmospheric precipitation indicates that the dissolved salts present in the water are a result of dissolved ions carried by rainfall rather than interaction with rocks (Gibbs, 1970) even though ion exchange and rock weathering may also contribute to the ionic concentration (Egbueri et al., 2019).

Approximately 60% of the water samples falls outside the boomerang field on the Cl ionic plot. This means the dominance

of precipitation extends towards lower TDS concentration at lower $Cl^-/Cl^- + HCO_3^-$ ratio. Some of the water plotted within the rock-water interaction regions (43% and 29% for Na^+ and Cl^- ionic ratios respectively), indicating that there is an interaction between the percolated water and the underground rock chemistry. These few groundwater samples falling within this region is an indication that geogenic origin is the leading factor responsible for ions increase from the precipitation domain towards the rock domain arising from water interacting with soils and possible weathering of rock forming minerals before getting to the top of the phreatic zone.

The groundwater samples generally have TDS values less than 100mg/L, except in one sample with 351mg/L, which signifies that they have low dissolved salts and low salinity. The amount of dissolved salts in water is controlled by precipitation which also affects the chemical composition of water with low-salinity (Gibbs, 1970; Egbueri et al., 2019). This possibly is responsible for most of the samples plotting in the precipitation dominance field on the Gibbs diagram. According to Gibbs (1970), the source of these types of chemistry is leaching from areas of low relief with low supply of dissolved salts, which is much greater in comparison to that supplied from rock dissolution, and high rainfall.

Hydrochemical processes

The Durov plot (Durov, 1948) is a composite diagram used in understanding the hydrochemical processes and the type of ion exchange in a hydrogeological environment. It consists of two ternary diagrams on which the cations and anions of interest that plots on an additional two-dimensional projection, known
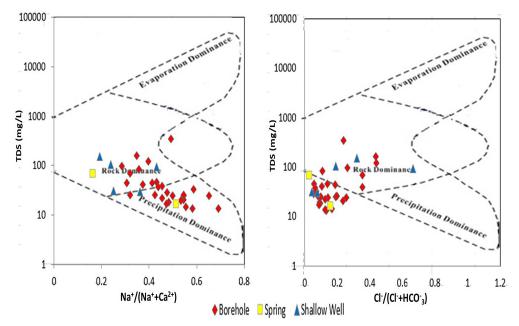
Figure 5. Mechanism of Groundwater Evolution on the Gibbs Diagram.

as the Durov's projection, which could be extended (extended Durov plot) with two binary plots for the TDS and pH (Lloyd & Heathcote, 1985) for better comparison. The diagram clusters the data points with similar chemical compositions and gives useful relationships and characteristics of large samples (Obeidat & Rimawi, 2017).

The extended Durov plot for the sampled wells is shown in Figure 6. Samples around the north-east and south-west regions (17%) fall within the mixing or dissolution zone, indicating that the major hydrogeochemical process here are mixing and simple ion exchange with no dominant cation-anion exchange which signifies fresh recent recharge to the aquifer. The other groundwater (83%), except the water from one, fall in the region of ion exchange in which Ca^{2+} replaces Na^+ and Mg^{2+}, implying more cation-anion exchange in them.

The major ions present in groundwater are useful in describing its evolution as it interacts with rocks and dissolves the carbonate and silicate minerals, leading to ion exchange processes (Aghazadeh et al., 2017). The major ions data and their relationship were plotted to know the hydrochemical evolution of the groundwater and processes operating in the aquifer of the study area (Figure 7). The ratio of Ca^{2+}/Mg^{2+} is commonly used to determine the source of calcium and magnesium ion into the groundwater system (Srinivasamoorthy et al., 2014). If Ca^{2+}/Mg^{2+} is equal to 1, it indicates dolomite dissolution; between 1 and 2 is calcite dissolution while greater than 2 means that silicate dissolution is responsible for Ca^{2+} and Mg^{2+} in the groundwater. Most of the samples (74%) plot above the ratio line 2 signifying the effect of silicate weathering in contributing Ca^{2+} into the groundwater. The other samples (26%) plot within the 1 and 2 ratio lines indicating increase in Mg^{2+} as a result of ion exchange with Na^+

The plot of alkalinity against Na shows that over 95% of the samples plotted below the equiline (1:1) indicating that silicate
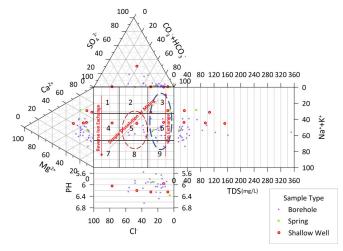

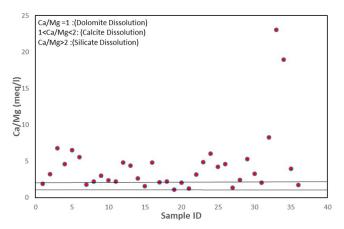**Figure 6.** Durov Diagram of the Groundwater Samples.

Figure 7. Ca^{2+}/Mg^{2+} Versus Samples Scatter Diagram for the Studies Samples.

weathering is dominant in the groundwater (Figure 8a). The higher concentration of Na is indicative of the influence of ion exchange processes. Only one sample plotted above the equiline which signifies possible anthropogenic signature. All samples plotted below the equiline for Ca +Mg against total cation and Na + K against total cation on the bivariate plots indicating that the cations are produced through ion exchange and silicate weathering (Figure 8b and 8c).

Enrichment or depletion of Na in relation to Cl is also useful in understanding the hydrochemical evaluation of groundwater. A 1:1 Na/Cl ratio indicates dominance of evaporation processes, especially from halite dissolution, if no mineral species are precipitated; a ratio greater than 1 signifies Na release through weathering of silicates from rock water interaction (Srinivasamoorthy et al., 2014; Aghazadeh et al., 2017) or cation exchange; while a ratio less than 1 is as a result of anthropogenic influence. Most of the samples (77%) plotted on or above the 1:1 ratio line while 23% plotted below the line, which suggests that Na^+ is mainly derived

from silicate weathering, halite dissolution and cation exchange between Na^+ and Ca^{2+} (Figure 8d). This also agrees with the result of the saturation index of halite (Figure 4a) which shows an undersaturated state for all samples.

The concentration of calcium in groundwater may increase as a result of dissolution of $CaCO_3$ and $CaMg(CO_3)_2$ from rocks as groundwater flows or during infiltration (Refat-Nasher & Humayan-Ahmed, 2021). On the bivariate plot of $Ca^{2+} + Mg^{2+}$ against $SO_4^{2-} + HCO_3$, ionic concentration plotting above the 1:1 line originate from ion exchange process due to an excess of $SO_4^{2-} + HCO_3$ while ionic concentration plotting below this line signify that the dominant process is reverse ion exchange arising from excess of $Ca^{2+} + Mg^{2+}$ over $SO_4^{2-} + HCO_3$. Over 70% of samples plotted near or slightly above the 1:1 line implying an origin from ion exchange processes of silicate and carbonate mineral weathering (Figure 8e). The other 30% falls far below the 1:1 line signifying reverse ion exchange process arising from calcite weathering and dissolution of gypsum.
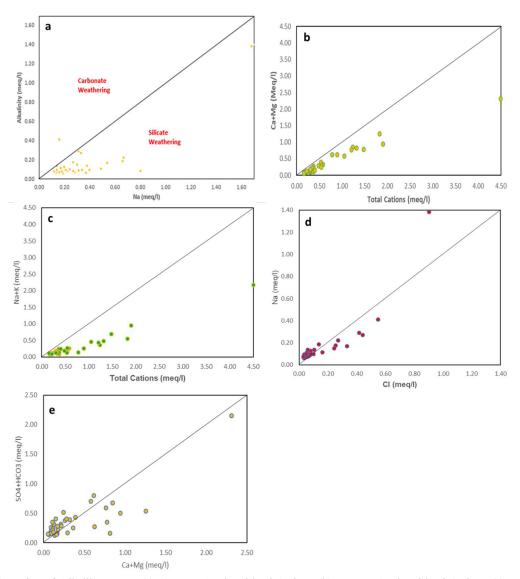

Figure 8. Bivariate plot of Alkaliity Vs Na (a); Ca+Mg Against Total Cations (b); Na+K Against Total Cations (c); Na vs Cl (d); and SO_4+HCO_3 vs Ca+Mg (e).

CONCLUSION

Various graphical methods and hydrogeochemical modelling were employed to understand the groundwater geochemistry and hydrochemical processes in the Egbako aquifer, with the following conclusions reached;

From statistical summary, the abundance of major cations in the ground water are $Ca^{2+} > K^+ > Na^+ > Mg^{2+}$ while the anion is $HCO_3^- > NO_3^- > Cl^- > SO_4^{2-} > NO_2^-$.the water samples are slightly acidic to alkaline with TDS below 1000mg/L and as such are considered as fresh water. The main hydrochemical facies are $Ca–HCO_3$, $Na–HCO_3$ and mixed Ca, Na, $Mg–HCO_3$. With the $Na-HCO_3$ facies believed to be anthropogenic influenced.

Groundwater plots on the Gibbs diagram reveals that the main controlling factor of the groundwater chemistry is atmospheric precipitation indicating that the dissolved salts present are a result of ions dissolution carried by rainfall together with ion exchange and rock weathering that may also contribute to the concentration of ions.

Saturation indices indicate that rock weathering which include dissolution of carbonates, evaporites and silicate minerals and to some extent, precipitation of kaolinite are important rock-water interactions affecting the evolution of the groundwater chemistry.

Hydrochemical modelling on the Durov diagram and graphical plots shows that silicate weathering and silicate dissolution is responsible for the presence of Na, Mg and Ca ion in the groundwater. The chemical composition of groundwater in the Egbako aquifer is dominantly controlled by ion exchange, simple dissolution, silicate weathering and some anthropogenic activities especially from agricultural activities.

ACKNOWLEDGEMENTS

REFERENCES

Adeleye, D. R. (1974). Sedimentology of the fluvial Bida Sandstones (Cretaceous), Nigeria. *Sedimentary Geology*, *12*(1), 1-24.

Aghazadeh, N., & Mogaddam, A. A. (2011). Investigation of hydrochemical characteristics of groundwater in the Harzandat aquifer Northwest of Iran. *Environmental Monitoring and Assessment*, *176*(1-4), 183-195. PMid:20625825. http://dx.doi.org/10.1007/s10661-010-1575-4.

Aghazadeh, N., Chitsazan, M., & Golestan, Y. (2017). Hydrochemistry and quality assessment of groundwater in the Ardabil area, Iran. *Applied Water Science*, *7*(7), 3599-3616.

Amadi, A. N., Olasehinde, P. I., Obaje, N. G., Unuevho, C. I., Yunusa, M. B., Keke, U. N., & Ameh, I. M. (2017). Investigating the Quality of Groundwater from Hand-dug Wells in Lapai, Niger State using Physico-chemical and Bacteriological Parameters. *Minna Journal of Geosciences*, *1*(1), 77-92.

Anurunwa, N. J., & Adesiji, A. R., & Agbese, E. (2020). Modelling runoff estimation in Bida Basin using improved soil moisture balance model. In *Proceedings of the 1st Civil Engineering Conference*. Minna, Nigeria: Department of Civil Engineering, Federal University of Technology.

Appelo, C. A. J., & Postma, D. (1993). *Geochemistry*. Rotterdam, the Netherlands: Balkema.

Ashafa, A., Saidu, M., & Gbongbo, J. (2020). Physico-chemical assessment of some selected hand dug wells water in Bida Metropolis, Niger State, Nigeria. In *Proceedings of the 2nd International Civil Engineering Conference*. Minna, Nigeria: Federal University of Technology.

Aweda, A. K., Jatau, B. S., Goki, N. G., Bashir, I. Y., & Obaje, N. G. (2023). Application of VES and 2D resistivity methods for groundwater exploration in Kutigi-Enagi Region, Northern Bida Basin, Nigeria. *Saudi Journal of Engineering and Technology*, *8*(2), 29-40. http://dx.doi.org/10.36348/sjet.2023.v08i02.001.

Deutsch, W. J. (1997). *Groundwater geochemistry: fundamentals and applications to contamination*. Boca Raton: CRC Press.

Durov, S. A. (1948). Classification of natural waters and graphic presentation of their composition. *Doklady Akademii Nauk SSSR*, *59*(1), 87-90.

Egbueri, J. C., Mgbenu, C. N., & Chukwu, C. N. (2019). Investigating the hydrogeochemical processes and quality of water resources in Ojoto and environs using integrated classical methods. *Modeling Earth Systems and Environment*, *5*(4), 1443-1461. http://dx.doi.org/10.1007/s40808-019-00613-y.

Fijani, F., Moghaddam, A. A., Tsai, F. T. C., & Tayfur, G. (2017). Analysis and assessment of hydrochemical characteristics of Maragheh-Bonab Plain Aquifer, Northwest of Iran. *Water Resources Management*, *31*(3), 765-780. http://dx.doi.org/10.1007/s11269-016-1390-y.

Gibbs, R. (1970). Mechanisms controlling world water chemistry. *Science*, *170*(3962), 1088-1090. PMid:17777828. http://dx.doi.org/10.1126/science.170.3962.1088.

Haile-Meskale, M. (2017). An overview of saturation state of groundwater with respect to some common minerals in South Central Ontario. *International Journal of Sciences, Basic and Applied Research*, *36*(5), 32-47.

He, X., Li, P., Shi, H., Xiao, Y., Guo, Y., & Zhao, H. (2022). Identifying strontium sources of flowback fluid and groundwater pollution using 87Sr/86Sr and geochemical model in Sulige gasfield,

China. *Chemosphere*, *306*, 135594. PMid:35803383. http://dx.doi.org/10.1016/j.chemosphere.2022.135594.

Idris-Nda, A. (2012). Estimating aquifer hydraulic properties in Bida Basin, Central Nigeria using empirical methods. *Earth-Science Reviews*, *2*(1), 209-221.

Idris-Nda, A., Ogunbajo, M. I., & Olasehinde, P. I. (2013). Determination of the aquifer system of the northern sector of Bida Basin, Nigeria using electrical resistivity method. *Journal of Geography and Geology*, *5*(2), 18-30.

Idris-Nda, A., Salihu, H. D., Jimada, A. M., & Babadoko, A. (2016). Groundwater quality in shallow unconfined sedimentary aquifers in Bida, Nigeria. In *Proceedings of the 39th WEDC International Conference Kumasi*, Ghana.

Idris-Nda, A., Abubakar, S. I., Waziri, S. H., Dadi, M. I., & Jimada, A. M. (2014). Groundwater development in a mixed geological terrain: a case study of Niger State, Central Nigeria. *Water Resources Management*, *8*, 77-87.

Kehinde, M. O. (1993). Preliminary isotopic studies in the Bida Basin, Central Nigeria. *Environmental Geology*, *22*(3), 212-217. http://dx.doi.org/10.1007/BF00767406.

Kogbe, C. A., Ajakaiye, D. E., & Matheis, G. (1983). Confirmation of rift structure along the Mid-Niger Valley, Nigeria. *Journal of African Earth Sciences*, *1*, 127-131.

Li, F., Wu, J., Xu, F., Yang, F., & Du, Q. (2023). Determination of the spatial correlation characteristics for selected groundwater pollutants using the geographically weighted regression model: a case study in Weinan, Northwest China. *Human and Ecological Risk Assessment*, *29*(2), 471-493. http://dx.doi.org/10.1080/10807039.2022.2124400.

Lloyd, J. A., & Heathcote, J. A. (1985). *Natural inorganic hydrochemistry in relation to groundwater: an introduction.* New York: Oxford University Press.

Mands, E. (1992). Kritische Betrachtung derWasserbilanzparameter und hydrologische Untersuchungen der Einzugsgebiete River Gbako und River Gurara (Mittelnigeria). *Giessener Geologische Schriften*, *47*, 1-174.

Mu, D., Wu, J., Li, X., Xu, F., & Yang, Y. (2023). Identification of the spatiotemporal variability and pollution sources for potential pollutants of the Malian River water in Northwest China Using the PCA-APCS-MLR receptor model. *Exposure and Health*. In press. http://dx.doi.org/10.1007/s12403-023-00537-0.

Nematollahi, M. J., Clark, M. J. R., Ebrahimi, P., & Ebrahimi, M. (2018). Preliminary assessment of groundwater hydrogeochemistry within Gilan, a northern province of Iran. *Environmental Monitoring and Assessment*, *190*(4), 242. PMid:29572684. http://dx.doi.org/10.1007/s10661-018-6543-4.

Nsabimana, A., & Li, P. (2023). Hydrogeochemical characterization and appraisal of groundwater quality for industrial purpose using a novel industrial water quality index (IndWQI) in the Guanzhong Basin, China. *Chemie der Erde*, *83*(1), 125922. http://dx.doi.org/10.1016/j.chemer.2022.125922.

Nsabimana, A., Wu, J., Wu, J., & Xu, F. (2023). Forecasting groundwater quality using automatic exponential smoothing model (AESM) in Xianyang City, China. *Human and Ecological Risk Assessment*, *29*(2), 347-368. http://dx.doi.org/10.1080/10807039.2022.2087176.

Obaje, N. G., editor. (2009). *Geology and mineral resources of Nigeria.* Berlin: Springer-Verlag Heidelberg.. http://dx.doi.org/10.1007/978-3-540-92685-6.

Obaje, N. G., editor. (2013). *Updates on the geology and mineral resources of Nigeria.* Nigeria: Onaivi Printing and Publishing Limited.

Obaje, N. G., Bomai, A., Moses, D., Ozoji, T. M., & Habu, S. (2019). New insights on the geology and petroleum systems of the Bida Basin and Sokoto Sector of the Iullemmedin Basin. In *Proceedings of the 2nd Summit on Research Activities in Nigeria's Frontier Basins*, Abuja, Nigeria.

Obeidat, A. M., & Rimawi, O. (2017). Characteristics and genesis of the groundwater resources associated with oil shale deposits in the Azraq and Harrana Basins, Jordan. *Journal of Water Resource and Protection*, *9*(2), 121-138. http://dx.doi.org/10.4236/jwarp.2017.92010.

Offodile, M. E. (2013). *Hydrogeology: groundwater studies and development in Nigeria* (3rd ed.). Nigeria: Mecon Geology and Engineering Services.

Olabode, T. O., Eduvie, M. O., & Olaniyan, I. O. (2012). Evaluation of groundwater resources of the Middle Niger (Bida) Basin of Nigeria. *American Journal of Environmental Engineering*, *2*(6), 166-173. http://dx.doi.org/10.5923/j.ajee.20120206.04.

Olaniyan, O., & Olobaniyi, S. B. (1996). Facies analysis of the Bida Sandstone formation around Kajita, Nupe Basin, Nigeria. *Journal of African Earth Sciences*, *23*(2), 253-256. http://dx.doi.org/10.1016/S0899-5362(96)00066-8.

Owor, M., Muwanga, A., Tindimugaya, C., & Taylor, R. G. (2021). Hydrogeochemical processes in groundwater in Uganda: a national-scale analysis. *Journal of African Earth Sciences*, *175*, 104-113. http://dx.doi.org/10.1016/j.jafrearsci.2021.104113.

Piper, A. M. (1944). A graphic procedure in the geochemical interpretation of water-analyses. *Transactions - American Geophysical Union*, *25*(6), 914-928. http://dx.doi.org/10.1029/TR025i006p00914.

Prasanna, M. V., Chidambaram, S., Hameed, A. S., & Srinivasamoorthy, K. (2010). Study of evaluation of groundwater in Gadilam basin using hydrogeochemical and isotope data. *Environmental Monitoring and Assessment*, *168*(1–4), 63-90. PMid:19609693. http://dx.doi.org/10.1007/s10661-009-1092-5.

Rahaman, M. A. O., Fadiya, S. L., Adekola, S. A., Coker, S. J, Bale, R. B., Olawoki, O. A., Omada, I. J., Obaje, N. G., Akinsanpe, O. T., Ojo, G. A., & Akande, W. G. (2019). A revised stratigraphy of the Bida Basin, Nigeria. *Journal of African Earth Sciences*, *151*, 67-81. http://dx.doi.org/10.1016/j.jafrearsci.2018.11.016.

Rao, N. S. (2017). Controlling factors of fluoride in groundwater in a part of South India. *Arabian Journal of Geosciences*, *10*(23), 524. http://dx.doi.org/10.1007/s12517-017-3291-7.

Refat-Nasher, N. M., & Humayan-Ahmed, M. (2021). Groundwater geochemistry and hydrogeochemical processes in the Lower Ganges-Brahmaputra-Meghna River Basin areas, Bangladesh. *Journal of Asian Earth Sciences*, *X6*, 100062. http://dx.doi.org/10.1016/j.jaesx.2021.100062.

Ren, X., Li, P., He, X., Su, F., & Elumalai, V. (2021). Hydrogeochemical processes affecting groundwater chemistry in the Central Part of the Guanzhong Basin, China. *Archives of Environmental Contamination and Toxicology*, *80*(1), 74-91. PMid:33146757. http://dx.doi.org/10.1007/s00244-020-00772-5.

Sidi, A. A., Waziri, M. N., Maji, A. T., Okunlola, I. A., Umar, A., & Waziri, S. H. (2016). Assessment of Chemical Quality of Water from Shallow Alluvial Aquifers in and around Badeggi, Central Bida Basin, Nigeria. *Journal of Earth Sciences and Geotechnical Engineering*, *6*(3), 133-145.

Srinivasamoorthy, K., Gopinath, M., Chidambaram, S., Vasanthavigar, M., & Sarma, V. S. (2014). Hydrochemical characterization and quality appraisal of groundwater from Pungar sub basin, Tamilnadu, India. *Journal of King Saud University. Science*, *26*(1), 37-52. http://dx.doi.org/10.1016/j.jksus.2013.08.001.

Srinivasamoorthy, K., Nanthakumar, C., Vasanthavigar, M., Vijayaraghavan, K., Rajivgandhi, R., & Chidambaram, S. (2009). Groundwater quality assessment from a hard rock terrain, Salem District of Tamilnadu, India. *Arabian Journal of Geosciences*, *4*(1-2), 91-102. http://dx.doi.org/10.1007/s12517-009-0076-7.

Suleiman, Y. M. (2014). Surface runoff responses to rainfall variability over the Bida Basin, Nigeria. *Journal of Environment and Earth Science*, *4*(3), 67-74.

Tarawneh, M. S., Janardhana, M. R., & Ahmed, M. M. (2019). Hydrochemical processes and groundwater quality assessment in North eastern region of Jordan Valley, Jordan. *HydroResearch*, *2*, 129-145. http://dx.doi.org/10.1016/j.hydres.2020.02.001.

World Health Organization – WHO. (2022). *Guidelines for drinking-water quality: fourth edition incorporating the first and second addenda* (4th ed.). Geneva: WHO.

Xu, D., Li, P., Chen, X., Yang, S., Zhang, P., & Guo, F. (2023). Major ion hydrogeochemistry and health risk of groundwater nitrate in selected rural areas of the Guanzhong Basin, China. *Human and Ecological Risk Assessment*, *29*(3-4), 701-727. http://dx.doi.org/10.1080/10807039.2022.2164246.

Xu, F., Li, F., Chen, W., He, S., Li, F., Mu, D., & Elumalai, V. (2022). Impacts of land use/land cover patterns on groundwater quality in the Guanzhong Basin of northwest China. *Geocarto International*, *37*(27), 16769-16787. http://dx.doi.org/10.1080/10106049.2022.2115153.

Zhang, B., Zhao, D., Zhou, P., Qu, S., Liao, F., & Wang, G. (2020). Hydrochemical characteristics of groundwater and dominant water-rock interactions in the Delingha Area, Qaidam Basin, Northwest China. *Water*, *12*(3), 836. http://dx.doi.org/10.3390/w12030836.

Zhou, X., Shen, Ye., Zhang, H., Song, C., Li, J., & Liu, Y. (2015). Hydrochemistry of the Natural Low pH Groundwater in the Coastal Aquifers near Beihai, China. *Journal of Ocean University of China*, *14*(3), 475-483. http://dx.doi.org/10.1007/s11802-015-2631-z.

Zhou, Y., Wu, J., Gao, X., Guo, W., & Chen, W. (2022). Hydrochemical background levels and threshold values of phreatic groundwater in the Greater Xi'an Region, China: spatiotemporal distribution, influencing factors and implication to water quality management. *Exposure and Health*, http://dx.doi.org/10.1007/s12403-022-00521-0.

Authors contributions

Abdulwahid Kolawole Aweda: Corresponding author, conceptualization, methodology, data collection and analysis, data interpretation, original manuscript writing, review and editing.

Benson Shadrach Jatau: Conceptualization, methodology, data analysis, data interpretation, manuscript review, supervision.

Nathaniel Gotar Goki: Conceptualization, methodology, data analysis, data interpretation, manuscript review, supervision.

Editor-in-Chief: Adilson Pinheiro

Associated Editor: Edson Cezar Wendland